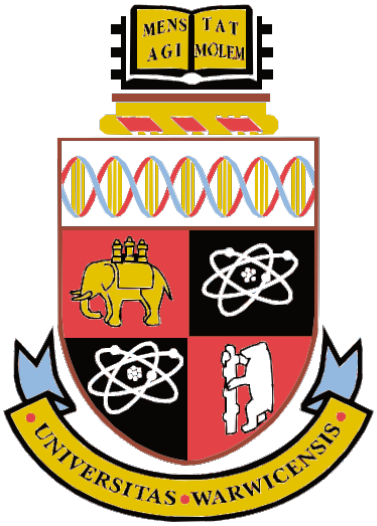

The Interfacial Dynamics of Bursting Bubbles

by

Lyllian Chanerley

MA4K9 Dissertation

Submitted to The University of Warwick

Mathematics Institute

April, 2025

Contents

1 Introduction

Bubbles within liquids are incredibly common, occurring in both a wide spectrum of natural and industrial processes [1, 2, 3, 4, 5, 6, 7, 8]. These occurrences can range from water and carbon-dioxide bubbles in magma providing driving forces for an eruption [1] to carbon-dioxide bubbles in champagne enhancing the evaporation of volatile organic compounds dispersed in the liquid phase. When a bubble rises to the surface of a liquid, it may burst, scattering many droplets. These droplets are an important process of transport exchange across the liquid gas interface[**?**], they are considered the main source of sea spray aerosols and impact air pollution[] as well as the transmission of infectious diseases[]. Bubbles formed due to the breaking of waves contribute to the transfer of heat, mass and other contaminants between the oceans and the atmosphere. The efficiency of this transfer is governed by the initial size and speed of the ejected drops.

There are two Phenomena that occur when a bubble bursts that produce aerosols, the first being when the thin film separating the bubble from the atmosphere is ruptured. The atomisation of the film can produce several hundred droplets of around a micrometer in diameter. Due to the length scales of the rupture being order O(100nm), we are unable to describe this problem with continuum mechanics. In fact, van der Waals forces or electrostatic repulsion must be considered, both of which are long-range intermolecular forces.

After the film rupture, the remaining cavity collapses causing a jet to form. This jet eventually breaches into one or more droplets. The key difference between these droplets and the droplets formed when the film ruptures is that they are much larger, order O(100μm) for a typical bubble with a diameter of a millimeter. They are also ejected vertically with a typical ejection velecity of order O(1ms^{-1}).

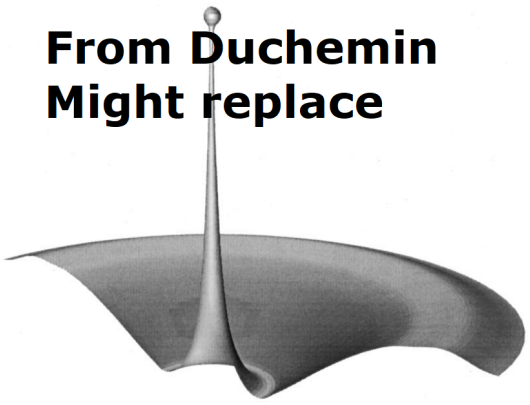

Figure 1: An image of jet formation due to a burst bubble

Literature review goes here:

just some notes:

$$We = \frac{\rho v^2 L}{\sigma}$$
$$La = \frac{\sigma \rho L}{\mu^2}$$
$$Re = \sqrt{LaWe}$$
$$Bo = \frac{\Delta \rho g L^2}{\sigma}$$
$$Oh = (La)^{-0.5})$$

2 Initial conditions

We need to determine the initial shape of a bubble floating at a gas-liquid interface before it's film ruptures. This derivation is based on the work done in [9]. We are considering the case where the fluid is stationary, i.e. $\mathbf{u} = \mathbf{0}$, meaning on the boundaries we only need to consider the Young-Laplace equation:

$$\Delta p = -\gamma \nabla \cdot \hat{n} \tag{1}$$

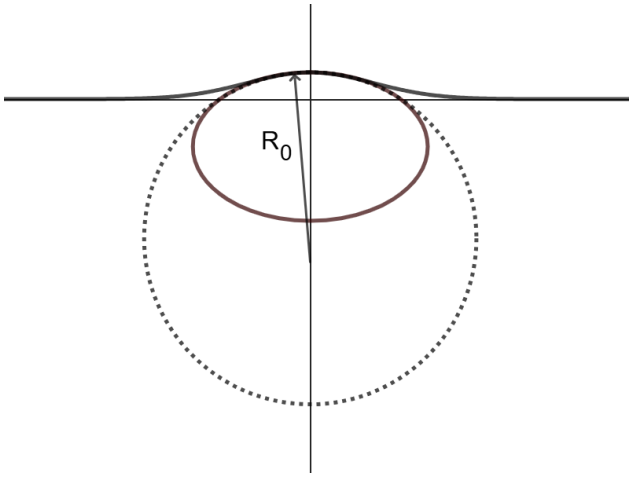

Figure 2: A bubble floating at a surface

We can divide the surface of a bubble into three regions: (A) the submerged portion of the interface, (B) the thin film over the top of the bubble separating the two gas regions, (C) the regions of the interface trailing away from the border of the thin film. We neglect the thickness of the film means we can ignore the weight of the film. Adding that the difference between the gas pressures inside and out of the bubble is uniform, the thin film

can be treated as a spherical surface of radius R_0. The force balance equations at any point on these surfaces are,

$$(\rho - \rho')gz = \gamma(\frac{1}{R_1} + \frac{1}{R_2} - \frac{4}{R_0}) \tag{2}$$

for region (A),

$$p = p_0 + \frac{4\gamma}{R_0} \tag{3}$$

for region (B),

$$(\rho - \rho')gz = \gamma(\frac{1}{R_1} + \frac{1}{R_2}) \tag{4}$$

for region (C) where γ represents surface tension of the liquid, g is acceleration due to gravity, ρ and ρ' are the densities of the liquid and gas respectively, p and p_0 are the gas pressure inside and outside the bubble respectively, g is acceleration due to gravity and z is the height above the still gas liquid interface in the far field. R_1 and R_2 are the principle radii of curvature of the surface at a point.

In order to calculate what R_1 and R_2 are we need to use some differential geometry. We assume the bubble can be described by a surfaces of revolution. Let Γ be a curve that lies in the plane (x, z) and let its equation have the equation $z = f(x)$. We then denote Φ as the surface defined by a rotation of Γ around the z-axis or axis of rotation. This surface can then be written in the form:

$$z = f(\sqrt{x^2 + y^2}) = f(r) \qquad\qquad r = \sqrt{x^2 + y^2} \tag{5}$$

Then using the formulas derived in [10] we get

$$E = 1 + (\frac{x}{r}f')^2, \qquad G = 1 + (\frac{y}{r}f')^2, \qquad F = \frac{xy}{r^2}(f')^2, \qquad EG - F^2 = 1 + (f')^2, \tag{6}$$

for the coefficients of the first fundamental form given by

$$I(\vec{\boldsymbol{\lambda}}) = E(\lambda_1)^2 + 2F\lambda_1\lambda_2 + G(\lambda_2)^2 \tag{7}$$

where λ is some tangent vector. We can exploit the fact that since our surface is radially symmetric, we only need to find these geometric characteristics on some meridian of the surface, say y=0:

$$E = 1 + (f')^2, \qquad\qquad G = 1, \qquad\qquad F = 0. \tag{8}$$

Again using the formulas in [10], we obtain

$$L = \frac{f''}{\sqrt{1+(f')^2}}, \qquad M = 0 \qquad N = \frac{f'}{x\sqrt{1+(f')^2}} \tag{9}$$

for the coefficients of the second fundamental form given by

$$II(\vec{\boldsymbol{\lambda}}, \vec{\boldsymbol{\mu}}) = L\lambda_1\mu_1 + M(\lambda_1\mu_2 + \lambda_2\mu_1) + N\lambda_2\mu_2. \tag{10}$$

We then obtain the principle curvatures κ_1 and κ_2 satisfy:

$$(EG - F^2)\kappa^2 - (EN + GL - 2MF)\kappa + LN - M^2 = 0. \tag{11}$$

Substituting in our coefficients for the first and second fundamental forms, solving for κ and noting radius of curvature is one over the curvature we obtain:

$$\frac{1}{R_1} = \kappa_1 = \frac{L}{E} = \frac{f''}{(1+(f')^2)^{\frac{3}{2}}}, \qquad \frac{1}{R_2} = \kappa_2 = \frac{N}{G} = \frac{f'}{x\sqrt{1+(f')^2}} \tag{12}$$

Notice that R_1 is exactly the radius of curvature of the meridian curve Γ We now introduce the variable ϕ defined to be the angle at which the tangent to Γ makes with the x-axis. We can calculate ϕ using simple trigonometry to be $\phi = \arctan(f'(x))$. We then consider:

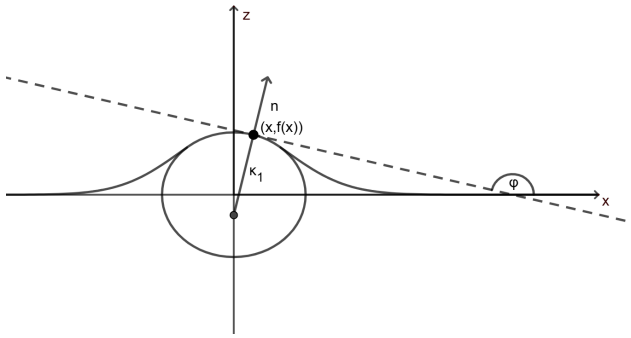

Figure 3: A bubble floating at a surface with a tangent line at a point. This tangent intersects the x-axis with angle ϕ

$$f'(x) = \tan\phi = \frac{\sin\phi}{\cos\phi} \tag{13}$$
$$= \sin\phi\sec\phi \tag{14}$$
$$= \sin\phi\sqrt{1+\tan^2\phi} \tag{15}$$
$$\frac{f'(x)}{\sqrt{1+f'(x)^2}} = \sin\phi \tag{16}$$
$$\frac{d}{dx}\frac{f'(x)}{\sqrt{1+f'(x)^2}} = \frac{d}{dx}\sin\phi \tag{17}$$
$$\frac{f''(x)}{(1+f'(x)^2)^{\frac{3}{2}}} = \frac{d(\sin\phi)}{dx} \tag{18}$$
$$\frac{1}{R_1} = \frac{d(\sin\phi)}{dx} \tag{19}$$

Allowing us to obtain R_1 in terms of ϕ. reparametrising the curve in terms of z, i.e. considering the curve given by $(g(z), z)$ where $g(z) = f^{-1}(z)$, we can find another expression for R_1. using the facts,

$$f'(x) = \frac{1}{g'(f(x))}, \qquad f''(x) = \frac{-g''(f(x))}{g'(f(x))^3} \tag{20}$$

We can write the curvature in terms of z:

$$\frac{f''(x)}{(1+f'(x)^2)^{\frac{3}{2}}} = \frac{-\frac{g''(f(x))}{g'(f(x))^3}}{(1+\frac{1}{g'(f(x))})} = \frac{-g''(f(x))}{(g'(f(x))^2+1)^{\frac{3}{2}}} = \frac{-g''(z)}{(g'(z)+1)^{\frac{3}{2}}} \tag{21}$$

Now we can consider,

$$f'(x) = \frac{1}{g'(f(x))} = \tan\phi = \frac{\sin\phi}{\cos\phi} \tag{22}$$
$$g'(z) = \cos\phi\csc\phi \tag{23}$$
$$= \sin\phi\sqrt{1+\cot^2\phi} \tag{24}$$
$$\frac{g'(z)}{\sqrt{1+g'(z)^2}} = \cos\phi \tag{25}$$
$$\frac{d}{dz}\frac{f'(z)}{\sqrt{1+f'(z)^2}} = \frac{d}{dz}\cos\phi \tag{26}$$
$$\frac{g''(z)}{(1+g'(z)^2)^{\frac{3}{2}}} = \frac{d(\cos\phi)}{dx} \tag{27}$$
$$\frac{1}{R_1} = -\frac{d(\cos\phi)}{dz} \tag{28}$$

We can also write R_2 in terms of ϕ by considering the normal to the curve at a point $(x, f(x))$. An equation for this normal is given by

$$(\bar{x} - x) + f'(x)(\bar{z} - f(x)) = 0 \tag{29}$$

where $(\bar{x}, \bar{z})$ are the coordinates of points on the straight line. We can the find the intersection of this line with the z-axis, $(0, \frac{x+ff'}{f'})$. Finding the distance R between this point and (x, f) gives

$$R = \sqrt{x^2 + (\frac{x + ff'}{f'} - f)^2} = \frac{x\sqrt{1 + (f')^2}}{|f'|} = R_2. \tag{30}$$

We can then use trigonometry to calculate R in terms of ϕ:

$$R = \frac{x}{\cos(\frac{\pi}{2} - \phi)} = \frac{x}{\sin(\phi)}. \tag{31}$$

Combining these all together we obtain

$$\frac{1}{R_1} = \frac{d(\sin(\phi))}{dx}, \tag{32}$$

$$\frac{1}{R_2} = \frac{\sin(\phi)}{x}, \tag{33}$$

$$\frac{dz}{dx} = \tan(\phi). \tag{34}$$

We now introduce a capillary constant a^2 having dimension of square length and defined

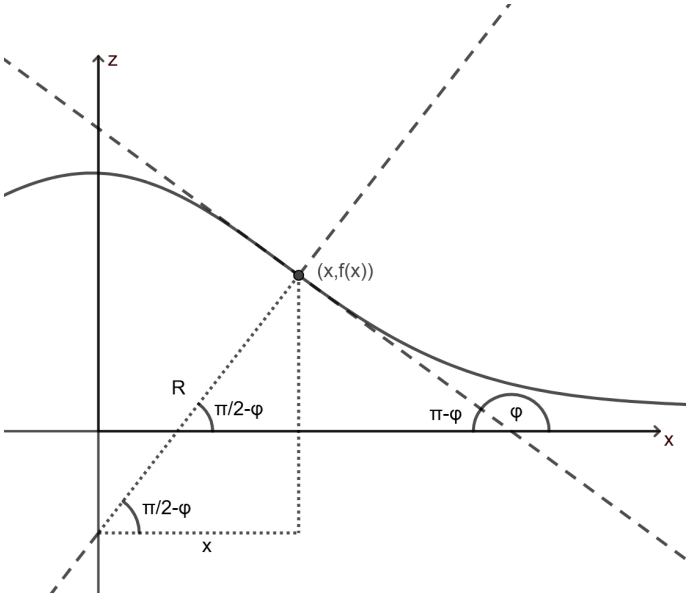

Figure 4: A bubble floating at a surface. Both a tangent line and a line normal to the curve are shown at a point. The distance along the normal between the point and the z-axis is given by R

by the equation

$$\frac{(\rho - \rho')g}{\gamma} = \frac{2}{a^2} \tag{35}$$

transform x, z, R_0, etc. to dimensionless quantities $\bar{x}$, $\bar{z}$, $\bar{R_0}$, etc. by

$$x = a\bar{x}, \qquad z = a\bar{z}, \qquad R_0 = a\bar{R}_0, \qquad \text{etc.} \tag{36}$$

We then consider two new transformed coordinates:

$$\bar{z}_1 = \bar{z} + \bar{h}, \qquad \bar{z}_2 = \bar{z} + \bar{l} \tag{37}$$

where $\bar{h}$ and $\bar{l}$ are chosen such that $\bar{z}_1$ has its origin at the deepest point of the bubble for portion (A) and $\bar{z}_2$ has its origin at the centre of the sphere for portion (B). For portion (A), instead of 2, we obtain

$$\left.\begin{aligned} \frac{d\bar{z}_1}{d\bar{x}} &= \tan\phi \\ \frac{d(\sin\phi)}{d\bar{x}} &= 2\bar{z}_1 - \frac{\sin\phi}{\bar{x}} + \theta \end{aligned}\right\} \tag{38}$$

or,

$$\left.\begin{aligned} \frac{d\bar{x}}{d\bar{z}_1} &= \cot\phi \\ \frac{d(\cos\phi)}{d\bar{z}_1} &= -2\bar{z}_1 + \frac{\sin\phi}{\bar{x}} - \theta \end{aligned}\right\} \tag{39}$$

where,

$$\theta = \frac{4}{\bar{R}_0} - 2\bar{h} \tag{40}$$

and the equations 38 and 39 are used for $\tan\phi < 1$ and $\tan\phi > 1$ respectively. Similarly for portion (C), equation 4 becomes,

$$\left.\begin{aligned} \frac{d\bar{z}}{d\bar{x}} &= \tan\phi \\ \frac{d(\sin\phi)}{d\bar{x}} &= 2\bar{z} - \frac{\sin\phi}{\bar{x}} \end{aligned}\right\} \tag{41}$$

We can notice that equation 38 and 39 are essentially the same of equation 41 except for the additional θ term. Finally equation 3 for portion (B) becomes

$$\bar{z}_2 = \sqrt{\bar{R}_0^2 + \bar{x}^2} \tag{42}$$

We are now ready to start solving for the initial condition.

2.1 Solving Portion (A)

We have derived the governing equations for each of the three portions of the bubble and now can start to solve them. We already have an explicit expression for portion (B),

although finding analytic solutions to 38, 39 and 41 is too difficult. Instead we can find numerical solutions using a Runge-Kutta method.

First we consider the equations 38 and 39. We use the initial conditions $\bar{x} = \bar{z}_1 = 0$ at $\theta = 0$ as we assume that at the bottom of the bubble is flat, i.e.

$$\frac{d\bar{z}_1}{d\bar{x}} = 0 \tag{43}$$

$$\Leftrightarrow \quad \theta = 0. \tag{44}$$

The relations

$$\frac{1}{\bar{R}_1} = \frac{\sin\phi}{\bar{x}} = \frac{1}{\bar{R}_2} = \frac{d(\sin\phi)}{d\bar{x}} = \frac{\theta}{2} \tag{45}$$

In order to solve this ODE, we used the `solve_ivp` function from SciPy [11]. Once again we need to do a little more work before we're able to use this function. First, consider the vector $\mathbf{z}$ defined by

$$\mathbf{z} = \begin{bmatrix} \bar{z}_1 \\ u \end{bmatrix} \tag{46}$$

where $u = \sin\phi$. Transforming our ODE we obtain

$$\frac{d\mathbf{z}}{d\bar{x}} = \begin{bmatrix} \frac{u}{\sqrt{1-u^2}} \\ -2\bar{z}_1 - \frac{u}{\bar{x}} + \theta \end{bmatrix} \tag{47}$$

which we can then solve for $\phi \in [0, \pi]$. As $\phi \to \pi/2$, $\frac{d\bar{z}_1}{dx} \to \infty$. This means our solver

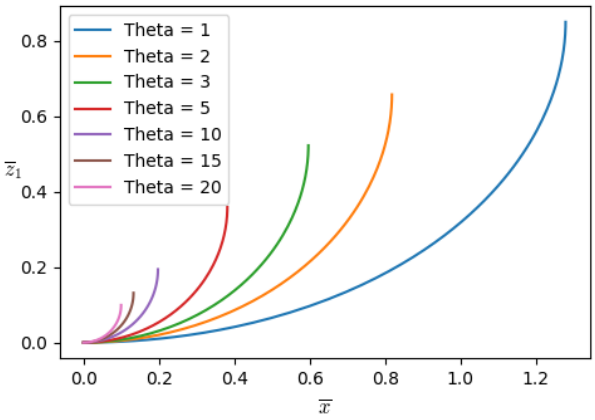

Figure 5: Solutions to 38 for various θ values

cannot compute the solution for $\phi > \pi/2$. What we do instead, is we can use the computed values for $\bar{z}_1$ and $\bar{x}$ at $\phi = \pi/2$ as initial conditions for equations 39. In a similar way to

before, we can transform the equations 39 into

$$\frac{d\mathbf{x}}{d\bar{z}_1} = \begin{bmatrix} \frac{v}{\sqrt{1-v^2}} \\ -2\bar{z}_1 + \frac{\sqrt{1-v^2}}{\bar{x}} - \theta \end{bmatrix}, \tag{48}$$

where $\mathbf{x} = \begin{bmatrix} \bar{x} \\ v \end{bmatrix}$ and $v = \cos\phi$. We can then once again use `solve_ivp` to get a full solution to 38 and 39.let this solution be denoted by the function F where

$$F(\bar{x}, \theta, \phi) = \begin{cases} f_1(\bar{x}, \theta) & \text{for } \phi > \pi/2 \\ \tilde{f}_1(\bar{x}, \theta) & \text{for } \phi < \pi/2 \end{cases} \tag{49}$$

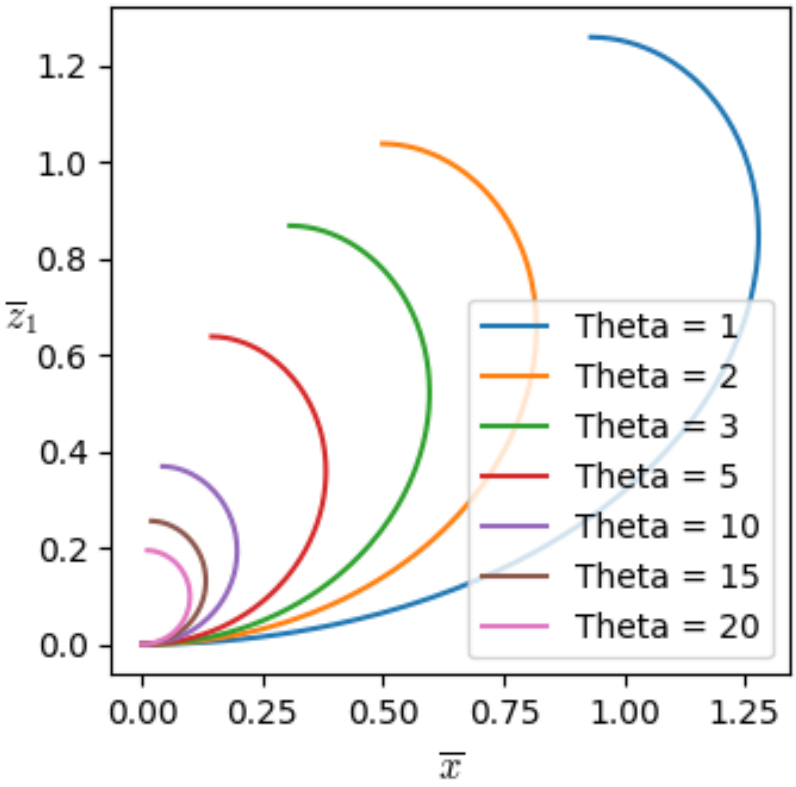

Figure 6: Solutions to 38 and 39 for various θ values

2.2 Solving Portion (C)

The equations generating portion (C) are very similar to portion (A), unfortunately, the boundary conditions make it much harder to solve. Portion (C) is the meniscus of the bubble and we would like it to flatten out at infinity. This means we have the boundary

conditions $\phi \to 0$, $\bar{z} \to 0$ as $x \to \infty$. These conditions are unable to be implemented numerically, instead we can consider initial conditions close to zero, i.e. $\bar{z} = \phi = 0.00001$ at $\bar{x} = \bar{x}_0$. We can then denote $\bar{z} = f_2(\bar{x}, \bar{x}_0)$ as a solution to 41

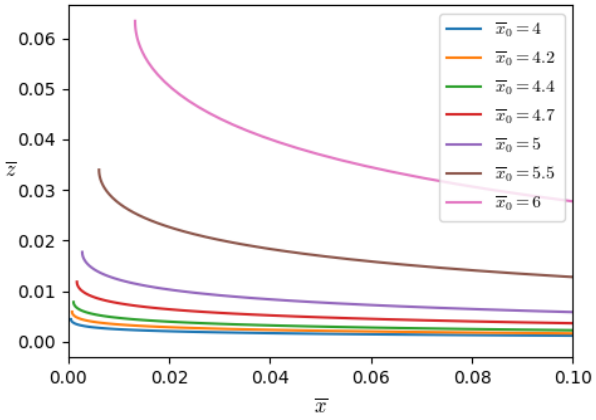

Figure 7: Solutions to 41 for various $\bar{x}_0$ values

2.3 Combining all the portions

We are now able to calculate an explicit description of the interface for each individual section, but we still have many unknown variables we need to solve for. We want each portion to meet at the same point and match derivatives at that point. applying these constraints we get the following system of equations:

$$\bar{z} = F(\bar{x}, \theta, \phi) - \bar{h} \tag{50}$$

$$\bar{z} = f_2(\bar{x}, \bar{x}_0) \tag{51}$$

$$\bar{z} = \sqrt{\bar{R}_0^2 - \bar{x}^2} - \bar{l} = f_3(\bar{x}, \bar{R}_0) - \bar{l} \tag{52}$$

$$\theta = \frac{4}{\bar{R}} - 2\bar{h} \tag{53}$$

and

$$\frac{d}{d\bar{x}} F(\bar{x}, \theta, \phi) = \frac{d}{d\bar{x}} f_2(\bar{x}, \bar{x}_0) = \frac{d}{d\bar{x}} f_3(\bar{x}, \bar{R}_0) \tag{54}$$

We can notice that $\frac{d}{d\bar{x}} f_3(\bar{x}, \bar{R}_0)$ is always negative and that $\frac{d}{d\bar{x}} F(\bar{x}, \theta, \phi)$ is only negative when $\phi > \pi/2$, i.e. when $F(\bar{x}, \theta, \phi) = f_1(\bar{x}, \theta)$. Using this we can reduce our system down to seven unknowns and six equations to solve, allowing us to have a free variable in θ

We can further reduce this highly non-linear system to two variables. For a fixed θ, we can consider this system in terms of $\bar{x}$ and $\bar{x}_0$ only. By fixing θ we can solve 39 and 38 to

obtain $f_1(\bar{x}, \theta)$. We can then solve 41 to obtain $f_2(\bar{x}, \bar{x}_0)$. We can then obtain

$$\bar{h} = f_1(\bar{x}, \theta) - f_2(\bar{x}, \bar{x}_0), \tag{55}$$

and

$$\bar{R}_0 = \frac{4}{2\bar{h} + \theta}. \tag{56}$$

Then we are able to calculate $f_3(\bar{x}, \bar{R}_0)$ and finally

$$\bar{l} = f_3(\bar{x}, \bar{R}_0) - f_1(\bar{x}, \theta). \tag{57}$$

This reduces out problem to finding the roots of

$$\frac{d}{d\bar{x}} f_1(\bar{x}, \theta) - \frac{d}{d\bar{x}} f_2(\bar{x}, \bar{x}_0) = 0 \tag{58}$$

$$\frac{d}{d\bar{x}} f_1(\bar{x}, \theta) - \frac{d}{d\bar{x}} f_3(\bar{x}, \bar{R}_0) = 0 \tag{59}$$

2.4 Solutions

We are now able to start

3 Conclusion

In summary, this has been a very successful project.

Bibliography

References

[1] Helge M Gonnermann and Michael Manga. The fluid mechanics inside a volcano. *Annu. Rev. Fluid Mech.*, 39(1):321–356, 2007.

[2] James C Bird, Riëlle De Ruiter, Laurent Courbin, and Howard A Stone. Daughter bubble cascades produced by folding of ruptured thin films. *Nature*, 465(7299):759–762, 2010.

[3] Luc Deike. Mass transfer at the ocean–atmosphere interface: the role of wave breaking, droplets, and bubbles. *Annual Review of Fluid Mechanics*, 54(1):191–224, 2022.

[4] Benjamin Dollet, Philippe Marmottant, and Valeria Garbin. Bubble dynamics in soft and biological matter. *Annual Review of Fluid Mechanics*, 51(1):331–355, 2019.

[5] Jie Feng, Matthieu Roché, Daniele Vigolo, Luben N Arnaudov, Simeon D Stoyanov, Theodor D Gurkov, Gichka G Tsutsumanova, and Howard A Stone. Nanoemulsions obtained via bubble-bursting at a compound interface. *Nature physics*, 10(8):606–612, 2014.

[6] Alexandros T Oratis, John WM Bush, Howard A Stone, and James C Bird. A new wrinkle on liquid sheets: Turning the mechanism of viscous bubble collapse upside down. *Science*, 369(6504):685–688, 2020.

[7] Fabrice Veron. Ocean spray. *Annual Review of Fluid Mechanics*, 47(1):507–538, 2015.

[8] Gérard Liger-Belair and Clara Cilindre. Recent progress in the analytical chemistry of champagne and sparkling wines. *Annual Review of Analytical Chemistry*, 14(1): 21–46, 2021.

[9] Yoshiaki Toba. Drop production by bursting of air bubbles on the sea surface (ii) theoretical study on the shape of floating bubbles. *Journal of the Oceanographical Society of Japan*, 15(3):121–130, 1959.

[10] Victor A Toponogov. *Differential geometry of curves and surfaces*. Springer, 2006.

[11] Pauli Virtanen, Ralf Gommers, Travis E. Oliphant, Matt Haberland, Tyler Reddy, David Cournapeau, Evgeni Burovski, Pearu Peterson, Warren Weckesser, Jonathan Bright, Stéfan J. van der Walt, Matthew Brett, Joshua Wilson, K. Jarrod Millman, Nikolay Mayorov, Andrew R. J. Nelson, Eric Jones, Robert Kern, Eric Larson, C J Carey, İlhan Polat, Yu Feng, Eric W. Moore, Jake VanderPlas, Denis Laxalde, Josef Perktold, Robert Cimrman, Ian Henriksen, E. A. Quintero, Charles R. Harris, Anne M. Archibald, Antônio H. Ribeiro, Fabian Pedregosa, Paul van Mulbregt, and

SciPy 1.0 Contributors. SciPy 1.0: Fundamental Algorithms for Scientific Computing in Python. *Nature Methods*, 17:261–272, 2020. doi: 10.1038/s41592-019-0686-2.

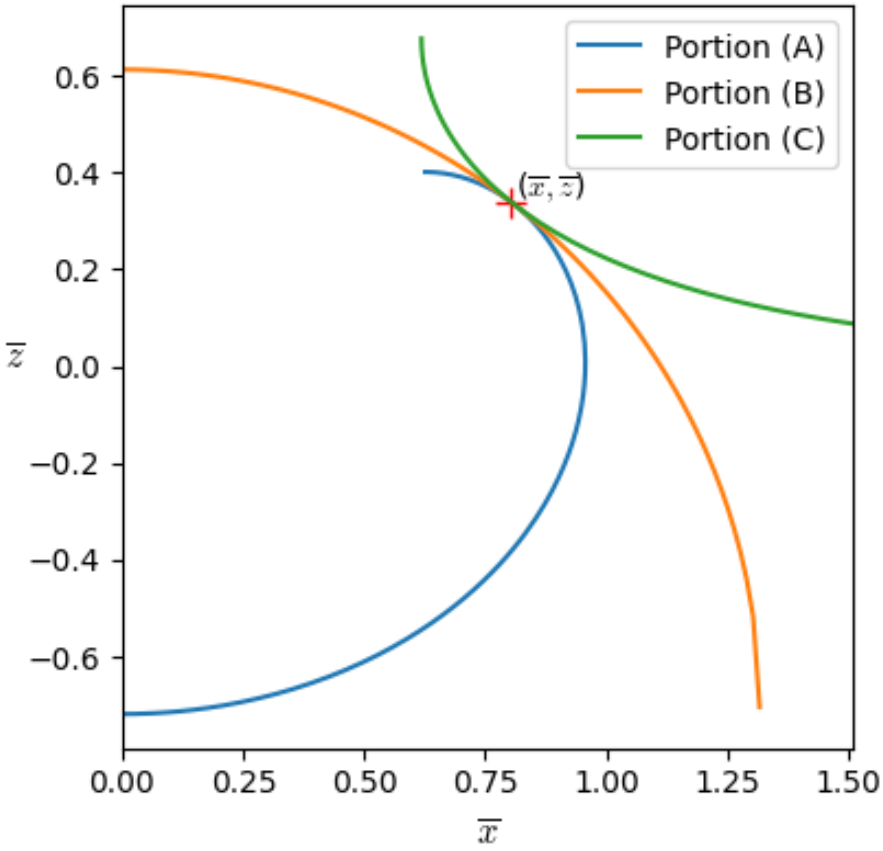

Figure 8: Solutions to full system for $\theta = 1.6$

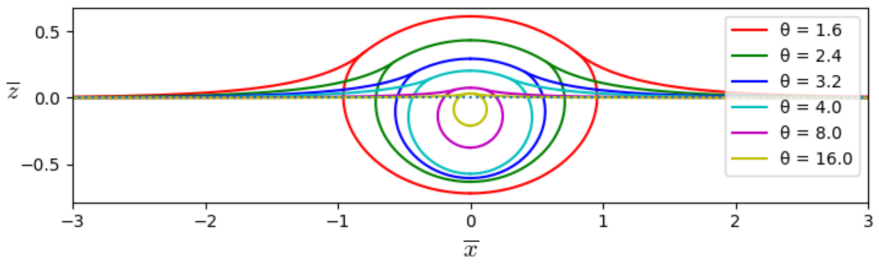

Figure 9: Solutions to full system for $\theta = 1.6, 2.4, 3.2, 4.0, 8.0, 16.0$

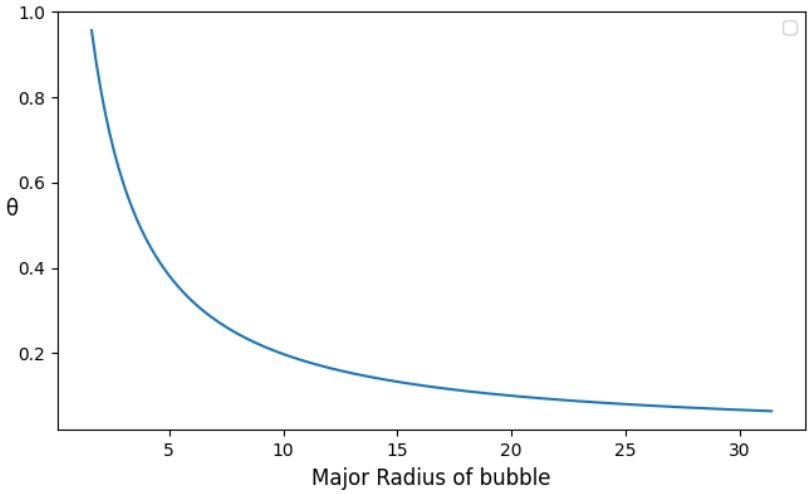

Figure 10: Size of the major radius of the bubble for varying values of θ